PHYSICAL REVIEW D VOLUME 18, NUMBER 2 15 JULY 1978

Spectrum of quantum chromodynamics in the limit of an infinite number of colors at fixed coupling

Richard Brower
Department of Physics, University of California, Santa Cruz, California 95064

Roscoe Giles and Charles Thorn
Center for Theoretical Physics, Laboratory for Nuclear Science and Department of Physics, Massachusetts Institute of Technology, Cambridge, Massachusetts 02139

(Received 29 March 1978)

We study quantum chromodynamics in the limit of an infinite number of colors N_c at fixed coupling g_s. On a null-plane lattice, the field theory can be recast as an interacting string model. The resulting dual string has internal degrees of freedom corresponding to the spin of the gluon quanta. The dynamics of these spins is that of an isotropic Heisenberg antiferromagnet. In the limit $N_c \to \infty$, low orders in the dual loop expansion are expected to give a good approximation to the spectrum (modulo effects such as spontaneous symmetry breakdown). We find that, in this limit, all particles lie on linear Regge trajectories. Quarkless gluonic states correspond to closed strings, and the spectrum is Lorentz invariant if the intercept of the leading trajectory is 2. Open strings are terminated by a quark and an antiquark, and the ρ trajectory must have intercept unity. Our limit preserves chiral symmetry: There is a $J^{PC} = 0^{++}$ scalar degenerate with the "pion" 0^{-+}. Both these particles are tachyons, so chiral symmetry may be spontaneously broken by string interactions. Our $N_c \to \infty$ calculations are similar to zero-temperature expansions in statistical mechanics. We expect them to give a *qualitatively* correct description of the ordered phase (confined quarks). We suggest that there is a critical number of colors below which confinement is lost. If $N_c = 3$ is close to this critical value (it is hoped, above it), the $1/N_c$ expansion might not give *quantitatively* accurate results.

I. INTRODUCTION

Understanding the spectrum and low-energy phenomenology of hadrons remains an outstanding problem in the context of local field theory. Though the popular candidate field theory of the strong interactions, quantum chromodynamics (QCD), may accurately describe hard processes involving few elementary quanta with large relative momenta, collective effects responsible for confinement and Regge behavior remain obscure. In light of successful phenomenological descriptions of hadrons as extended objects such as bags or strings, it is of some interest to pursue the question of how collective degrees of freedom describing such objects might arise in field theory.

Recently, a method has been devised for casting ordinary field theory in the language of interacting string theory.[1,2] In this scheme the sum of Feynman graphs for the field theory defined on a novel lattice in light-cone variables is reorganized as a sum of interacting lattice string graphs.[3] This is essentially a *kinematical* result. Each Feynman graph may be alternatively interpreted as describing interactions among field quanta or as describing latticized strings interacting by breaking or joining. It remains a *dynamical* question whether low-order perturbation theory either in the field theory or in the corresponding string theory accurately describes the full system.

If the dual loop expansion is to yield an accurate description of the theory, nonplanar graphs must be suppressed and quanta with infinitesimal momenta must interact strongly. In a theory like $\lambda\phi^4$ theory[1,2] there is no *a priori* reason for nonplanar graphs to be suppressed. Low-momentum quanta are expected to interact strongly in an infrared-unstable theory. In $\lambda\phi^4$ theory this will be the case only if $\lambda < 0$, for which the Hamiltonian is unbounded from below.

Quantum chromodynamics, being an infrared-unstable theory, is an ideal candidate for a string theory. Furthermore, as pointed out by 't Hooft,[4] nonplanar graphs can be suppressed by considering a large gauge group, i.e., a large number of colors N_c. In this paper, we discuss the string reinterpretation of QCD in the limit $N_c \to \infty$. Whether $N_c = 3$ is sufficiently large for our description to be accurate for real hadrons is an open question. The string interpretation also requires that the effective planar coupling $N_c g^2$ be large. Thus we may characterize our calculational scheme more concisely by saying that we are working in the limit of an *infinite number of colors at fixed coupling*.

In the $N_c \to \infty$ limit, the spectrum of the lattice theory is expected to be well approximated by that of planar fishnet graphs of transverse gluons interacting at four-point vertices. The space-time structure of such graphs is identical to that of the corresponding graphs in neutral $\lambda\phi^4$ theory and re-

produces the transverse excitations of the conventional string in the continuum limit. For $N_c \to \infty$, color excitations are "frozen" out and quark loops are suppressed, so that the only internal degrees of freedom of the corresponding strings are those deriving from the gluon spin. The dynamics of gluon-spin excitations of the $N_c \to \infty$ QCD string is identical to that of one of the two-dimensional ferroelectric models discussed by Giles, McLerran, and Thorn[5] in connection with the string representation of charged ϕ^4 theory.

For large N_c and $N_c g_s^2$, only states corresponding to closed strings (pure gluon) and open strings terminated by quark-antiquark interactions have finite energy in the continuum limit. The closed-string spectrum is identical to one of the spectra derived in Ref. 3. The effect of quarks on the ends of an open string is to polarize the spins of the neighboring gluons in such a way that the total spin of the ground state is zero. This state is a chiral doublet with tachyonic mass. This suggests the possibility of chiral-symmetry breakdown. The excitation spectra of both closed and open strings have linear Regge trajectories and are typical of a dual model in the zero-width approximation.

Just as in the generalized Veneziano model and the Neveu-Schwarz-Ramond model, our QCD string has a "graviton" in the closed-string sector and a "photon" in the open-string sector. The graviton is a spin-two state with no helicity ± 1 components and the photon is a spin-one state with no helicity-zero components, and Lorentz invariance demands that both these states be massless. If interactions are ignored this requirement fixes possible constants added to all (mass)^2 values in either sector.

We expect, however, that the breaking and joining interactions allowed to first order in $1/N_c$ will not be consistent[3] unless this additive constant is that determined by duality[3,6] or by a careful zero-point-energy calculation.[7] This value is proportional to the number of sets of bosonic oscillators characterizing the string spectrum. Unfortunately, the graviton and photon will be massless only if there are six sets of oscillators, whereas QCD in the $N_c \to \infty$ limit in four space-time dimensions yields only three: two for the transverse coordinates plus one for the gluon spin. Our interpretation of this inconsistency is that the $N_c \to \infty$ limit has frozen out too many degrees of freedom. For finite N_c, some degreees of freedom will presumably melt. It is also conceivable that another large-N limit such as the limit $N_c, N_f \to \infty$ with N_c/N_f fixed,[8] where N_f is the number of light flavors, may be consistent in four space-time dimensions.

The rest of this article is organized as follows: In Sec. II, we present and discuss the Feynman rules for QCD in the light-cone gauge. In Sec. III, we calculate the appropriate fishnet graphs for closed and open strings in QCD and present a discussion of the spectra in the two sectors. In Sec. IV we present concluding remarks.

II. FEYNMAN RULES FOR QCD IN LIGHT-CONE GAUGE

In this section we give the Feynman rules for QCD in a form most convenient for the null-plane lattice formulation of the theory that follows. Two ingredients are crucial: (i) The color indices for the SU(N_c) gauge group are arranged so that the powers in $1/N_c$ correspond to the dual topological classification of diagrams as emphasized by 't Hooft[4] and Veneziano,[8] and (ii) the standard light-cone variables

$$x^{\pm} = \frac{x^0 \pm x^3}{\sqrt{2}} , \tag{2.1a}$$

$$\vec{x}_\perp = (x^1, x^2) \tag{2.1b}$$

are used to make contact with the quantized string (in $\tau = ix^+$, $\sigma = P^+$ variables) of GGRT.[9]

We begin with the standard QCD Lagrangian

$$\mathcal{L} = \tfrac{1}{4} G_{\mu\nu i}{}^{j} G^{\mu\nu}{}_{j}{}^{i} + \bar{q}_a^i (i\not{D}_i{}^j - M_a \delta_i{}^j) q_j^a \tag{2.2}$$

for the anti-Hermitian matrix ($i, j = 1, \ldots, N_c$) gluon field

$$A^{\dagger}_{\mu i}{}^{j} = -A_{\mu j}{}^{i} , \tag{2.3}$$

where

$$G_{\mu\nu} \equiv \partial_\mu A_\nu - \partial_\nu A_\mu + g_s [A_\mu, A_\nu] , \tag{2.4}$$

$$D_\mu \equiv \partial_\mu + g_s \tilde{A}_\mu , \tag{2.5}$$

and for the quark q_{ai} (and antiquark $\bar{q}^{aj}$) fields with color indices ($i, j = 1, \ldots, N_c$) and flavor indices ($a = 1, \ldots, N_f$). To facilitate $1/N_c$ counting, the trace $A_{\mu k}{}^{k}$ is treated as an auxiliary (free) field that is explicitly decoupled by the use of

$$\tilde{A}_{\mu i}{}^{j} = A_{\mu i}{}^{j} - \frac{1}{N_c} \delta_i{}^j A_{\mu k}{}^{k} \tag{2.6}$$

in the definition of D_μ.

We now present the Feynman rules quantized in the light-cone gauge

$$A^+ = \frac{A^0 + A^3}{\sqrt{2}} = 0 , \tag{2.7}$$

which follow from a by-now-standard procedure.[10]

Following 't Hooft,[4] the color indices can be dealt with immediately. The (planar) gluon propagator is diagonalized in the color indices

$$\Delta^{\mu\nu}{}_{ij}{}^{i'j'} = \delta_i{}^{i'} \delta_j{}^{j'} \Delta^{\mu\nu}(P) \tag{2.8}$$

as represented in Fig. 1a by the two solid lines (or strip). Similarly the (planar) quark propagator,

$$D_i{}^{i'}{}_a{}^{a'}(P) = \delta_i{}^{i'}\delta_a{}^{a'}D(P) \tag{2.9}$$

is diagonal in color (solid line) and flavor (dashed line) indices (see Fig. 1b). Likewise, (planar) vertices have oriented indices connected by Kronecker δ's. The indices are indicated in Fig. 1c–e for the four-gluon (V_4), the three-gluon (V_3), and the one-gluon-quark (V_1) vertices. The singlet gluon-quark piece of V_1 removes the trace $A_{\mu k}{}^{k}$ field, but it is nonleading in $1/N_c$.

A consequence of utilizing these planar vertices and propagators is that for *each* Feynman diagram, we must add up all the interchanges of the indices (twists) to get the full contribution. However, gauge invariance only requires that each color line is connected to form a closed loop or trace. Thus we see, as noticed by 't Hooft, that the *only* effect of color and flavor for a diagram with c closed color loops and f closed flavor loops is an extra factor of $(N_c)^c(N_f)^f$. As discussed in the literature, the dual topological classification of diagrams is an immediate consequence.[4] For our purposes we only need to notice that for a given order in g_s^2 the dominant diagram as $N_c \to \infty$ is *planar* with *no* internal quark loops.

The momentum dependence of the propagators is

$$\Delta^{\mu\nu}(P) = \frac{i}{P^2 + i\epsilon}\left(g^{\mu\nu} - \frac{P^\mu g^{\nu+} + P^\nu g^{\mu+}}{P^+}\right), \tag{2.10}$$

$$D(P) = \frac{i(\gamma\cdot P + M)}{P^2 - M^2 + i\epsilon}, \tag{2.11}$$

where $\Delta^{\mu+} = 0$ due to our choice of gauge. These propagators couple to the standard vertices [Fig. 1(c)–(d)]:

$$V_4 = ig_s^2(2g_{\rho\mu}g_{\sigma\nu} - g_{\mu\sigma}g_{\nu\rho} - g_{\mu\nu}g_{\rho\sigma}), \tag{2.12a}$$

$$V_3 = ig_s[g_{\rho\nu}(k-q)_\mu + g_{\rho\mu}(P-k)_\nu + g_{\mu\nu}(q-P)_\rho], \tag{2.12b}$$

$$V_1 = ig_s\gamma_\mu. \tag{2.12c}$$

We may also separate the gluon into its transverse (A_i, $i=1,2$) and longitudinal (A_μ, $\mu=+$) pieces. Since $\Delta^{\mu+}=0$ and $g_{++}=0$, we see that the four-gluon vertex *never* transmits longitudinal gluons, and thus

$$\Delta^{ij} = \delta^{ij}\frac{(-i)}{P^2 + i\epsilon} \tag{2.13}$$

is the only term in the propagator which couples to these vertices.

For the analysis of Sec. III, we need the Feynman rules expressed in the variables $\tau = ix^+$, P^+, $\vec{x}$, i.e., we must Fourier transform the variables P^- and $\vec{P}$. The gluonic fishnet graphs we calculate in Sec. III involve only transverse gluons and the V_4 vertices. Since there are no factors of momentum either in the V_4 vertices or in the transverse gluon propagator numerators, for these graphs this transformation is precisely the same as in neutral scalar theory[1,2]:

$$-\Delta^{ij}(\tau, \vec{x}_\perp, P^+) = \delta^{ij}\frac{\theta(P^+\tau)}{4\pi P^+}\left(\frac{P^+}{2\pi\tau}\right)\exp\left(-\frac{P^+}{2\tau}\vec{x}_\perp{}^2\right). \tag{2.14}$$

As we shall see in Sec. III, the gluon-spin dependence of these graphs will yield a 6-vertex ferroelectric model.[5]

The transformation to light-cone variables for the fishnet graphs involving quark lines is more complicated, because the fermion propagator has momentum factors in the numerator. In particular there is a $P_\perp, P^-$ independent piece of the fermion propagator whose fourier transform is proportional to

$$\gamma^+\delta(\tau)\delta(\vec{x}_\perp), \tag{2.15}$$

which, when sandwiched between two transverse gluon vertices, gives a "seagull"-like structure. In Sec. III, we shall see that the strong-coupling fishnet diagram involving one quark line and one antiquark line contains only these seagull vertices. The only nonzero piece of a fermion propagator sandwiched between two such seagull vertices is the piece

$$\frac{i\gamma^- P^+}{P^2 - M^2 + i\epsilon}, \tag{2.16}$$

so for these graphs the transformation to τ, $\vec{x}_\perp$ variables again is very like $\lambda\phi^4$ theory.

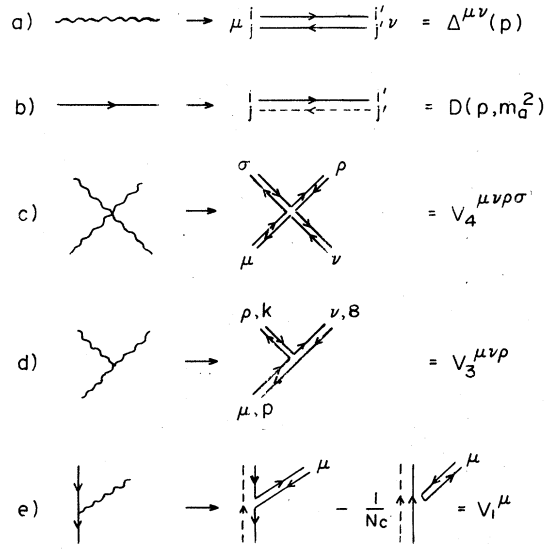

FIG. 1. The "planar" propagators and vertices with clockwise orientation of color flow. Solid lines indicate Kronecker δ functions $\delta_i^{i'}$ for color and dashed lines indicate Kronecker δ functions $\delta_a^{a'}$ for flavor.

In order to systematically carry out the transformation for quark lines, it is easiest to go back to the Lagrangian and recognize that the quark field can be written

$$q = q^{(+)} + q^{(-)}, \tag{2.17a}$$

where

$$q^{(-)} = \frac{\gamma^-\gamma^+}{2} q \tag{2.17b}$$

and

$$q^{(+)} = \frac{\gamma^+\gamma^-}{2} q\,. \tag{2.17c}$$

The $q^{(+)}$ variables do not involve derivatives with respect to x^+, so they can be explicitly integrated out.[11]

The result of this procedure is an effective quark Lagrangian involving only the two component $q^{(-)}$ fields:

$$\mathcal{L}^{\text{effective}}_{\text{quarks}} = i q^{(-)\dagger}\left(\frac{1}{2}\frac{\vec{\partial}}{\partial x^+} + g_s A_+\right) q^{(-)} + \frac{i}{2} q^{(-)\dagger}(i\gamma^j\partial_j - i g_s \vec{\gamma}\cdot\vec{A} + M)\frac{1}{2}\left(\frac{1}{\vec{\partial}_-} - \frac{1}{\vec{\partial}_-}\right) \times (i\gamma^j \vec{\partial}_j + i g_s \vec{\gamma}\cdot\vec{A} + m) q^{(-)}. \tag{2.18}$$

From this effective Lagrangian we read off the (two component) quark propagator

$$\frac{+i2P^+}{P^2 - m^2 + i\epsilon} \tag{2.19}$$

and the quark-antiquark seagull vertex (see Fig. 2)

$$i g_s^2 \left(-\frac{1}{2Q^+}\right)\gamma_i\gamma_j \tag{2.20}$$

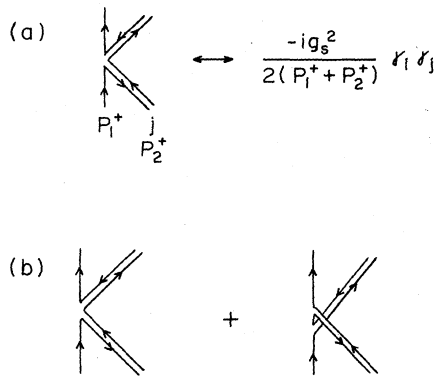

FIG. 2. (a) The planar representation for the quark-gluon "seagull" for light-cone quantization. (b) Two seagull contributions to quark-gluon scattering. When inserted in larger graphs, the second will be order $1/N_c$ compared to the first.

where Q^+ is the total Q^+ carried by the quark and adjacent gluon. We also observe that the trilinear quark-antiquark-gluon vertex involves transverse coordinate derivatives, and we do not extract its structure, as it will not be needed in the remainder of this paper.

The spin structure of the quark seagull vertex is amusing in the limit $N_c \to \infty$. First, notice that there can be no flip of S^z between the gluon line and the quark line. This is obvious because the gluon spin flip must be ±2 units and the quark spin flip must be ±1 units. Secondly, in quark-gluon scattering in the $N_c \to \infty$ limit, the dominant seagull vertex is the one where the quark and incoming gluon are adjacent in the sense of ordering of γ matrices [see Fig. 2(b)]. Clearly, this vertex will be nonzero only if the incoming quark and gluon spins are antialigned: the interaction involving parallel incoming spins is down by $1/N_c$ since the gluon must couple to the nonadjacent γ matrix.

We close this section with a brief discussion of the remaining vertices, which will not occur in the leading fishnet graphs calculated in Sec III. The trilinear vertex involving three transverse gluons will be complicated by transverse coordinate derivatives but is otherwise straightforward. The one involving two transverse and one longitudinal gluons requires a bit more discussion, because the propagator for the longitudinal gluon

$$\Delta^{--} = \frac{i}{(P^+)^2} + \frac{i\vec{P}^2}{(P^2 + i\epsilon)(P^+)^2} \tag{2.21}$$

has a piece independent of $P_\perp$ and P^-. Thus, its Fourier transform will be proportional to

$$\delta(\tau)\,\delta(\vec{x}_\perp), \tag{2.22}$$

so that two three-gluon vertices joined by this piece of the propagator will have the space-time structure (in x^+ and $\vec{x}_\perp$) of the four-gluon interaction. In fact, in a similar fashion as in the treatment of the corresponding problem in the case of fermions, the easiest way to handle systematically the longitudinal gluon is to go back to the Lagrangian and recognize that it is free of x^+ derivatives of A^-, so A^- can be integrated out. Alternatively, one can identify the induced vertices by separating from our propagators [Eqs. (2.10)–(2.11)] the "instantaneous" pieces that contribute as $P^- \to \infty$. It is useful to note that the induced four-gluon and $2g$-two-quark vertices only involve transverse gluons and not $P_\perp$ factors. This gives a decoupling of the spin and orbital dependence in a particular Lorentz frame which accounts for the factorization of the spin dynamics from the orbital dynamics. Moreover, no higher-point

vertices are induced.

We shall not go into the details of this procedure except to mention a caveat associated with the spurious singularities at $P^+=0$ in this gauge. These singularities are gauge artifacts and are presumably not present in gauge-invariant quantities. This has been demonstrated in great detail in the case of two-dimensional QCD,[12] and we expect no special trouble in four dimensions. It is important, however, in a specific calculational framework, which uses non-gauge-invariant quantities in intermediate stages of the calculations, to regulate these singularities in a systematic manner. One possibility is a principal-value prescription.[12] Our calculational framework utilizes a lattice in P^+, so we have a natural regulator, namely simply to exclude the $P^+=0$ mode. But this we describe in more detail in the following section.

III. THE SPECTRUM OF BARE STRINGS IN QCD

The string representation of QCD emerges clearly when the field theory is regulated via the introduction of a two-dimensional lattice in the light-cone coordinates τ and P^+. In each graph, we replace integrals over τ and P^+ by sums over discrete variables:

$$\tau = ka, \quad k = 1, 2, \ldots, \qquad P^+ = lb, \quad l = 1, 2, \ldots . \tag{3.1}$$

As was the case in the ϕ^4 theory discussed in Ref. 2, this prescription results in quark and transverse-gluon propagators and vertices which are dependent only on the ratio of lattice spacings $T_0 \equiv b/a$, which will be identified as the string tension $1/2\pi\alpha'$.

In $\lambda\phi^4$ theory, the exclusion of $\tau=0$ and $P^+=0$ from the lattice sums served as ultraviolet and infrared cutoffs, respectively. In particular, the exclusion of $P^+=0$ can be seen to correspond, in the continuum limit, to a principal-value prescription for performing integrations over the light-cone measure dP^+/P^+. In the scalar theory, the correct field-theory infrared structure is recovered in the continuum limit as an effect due to the summation over large numbers of lattice modes near $P^+=0$.

The $P^+=0$ singularities of the QCD Feynman rules are more severe and more subtle. As we have seen in Sec. II, the longitudinal gluon propagator has an extra factor $1/P^+$ relative to that of the transverse modes. It can readily be seen that this is related to our incomplete specification of gauge ($A^+=0$), which leaves a residual group of x^--independent gauge transformations. In our Fourier representation these affect only the longitudinal $P^+=0$ mode. For the present, we exclude $P^+=0$ longitudinal exchanges from the lattice theory. The question of whether, by summation over modes near $P^+=0$, we recover the correct residual gauge invariance in the continuum limit is not fully answered.[13]

In the cutoff lattice theory we have now defined, we note that, as discussed in Ref. 2, there are only a finite number of graphs for any Green's function carrying finite P^+ over finite τ. Because each propagator is Gaussian in the transverse coordinates of its end-point vertices, integrals over the transverse coordinates are finite. Therefore, the lattice theory has no divergences.

For $N_c \to \infty$, g_s^2 fixed on the lattice, the dominant graphs are those with the maximum possible number of gluon four-point vertices arranged in a planar configuration. Each gluon line carries the minimum $P^+=b$ and propagates the minimum time $\Delta\tau = a$. Graphs with three-point vertices or closed quark loops are all down by powers of N_c. Within the set of dominant fishnet graphs, at a given total $P^+=Mb$, there are several topologies which are of the same order in N_c. These correspond to the propagation of one or more disconnected cylindrical fishnet graphs or of a planar fishnet graph terminated by quark-antiquark interacting with the gluons via the seagull graph discussed in Sec. II. Planar fishnet graphs terminating in gluons are suppressed by one power of $N_c g_s^2$ per time step.

The Feynman amplitudes corresponding to cylindrical and planar gluon fishnet graphs are interpreted as functional integrals describing the propagation of bare (noninteracting) closed and open strings[2] (see Fig. 3). Graphs in which disconnected fishnets merge or in which a fishnet splits are down by a power of N_c for each point of splitting or joining and will be considered as interactions among the strings described. Each such amplitude is a product of integrals over the transverse coordinates of vertices and sums over the color and spin degrees of freedom of the gluon "links" of the fishnet. The factor arising from transverse coordinate integrals is precisely that encountered in

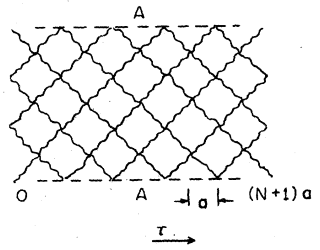

FIG. 3. A fishnet graph reprsenting the propagator of a single closed string. Vertices on the lines labeled "A" are to be identified.

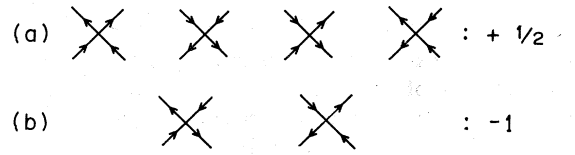

FIG. 4. The spin-vertex weights of the QCD fishnet graph. The four vertices in (a) have net polarization in a planar channel, those in (b) do not.

ϕ^4 theory and describes the propagation of a neutral string. Because the $N_c \to \infty$ limit freezes out the color degrees of freedom and leads only to an overall factor N_c^A where A is the number of unit cells in the fishnet, the only nontrivial internal symmetry structure is that due to excitations of the transverse gluon spin degrees of freedom.

Each link has two possible transverse spin states. Four spins are coupled at a vertex with the factor

$$\delta_{i_1 i_3}\delta_{i_2 i_4} - \tfrac{1}{2}(\delta_{i_1 i_2}\delta_{i_3 i_4} + \delta_{i_1 i_4}\delta_{i_2 i_3}) .$$

It is convenient to characterize the spin state of a link by its z component and to represent the two possible orientations of each link by an appropriately directed arrow. The possible vertices and their associated weights are as shown in Fig. 4. Note that, aside from the negative sign of some of the vertex weights, the internal spin dynamics are identical to those of the statistical-mechanical "F model"[14] (see Fig. 5), the analysis of which has been done in Pef. 5.

For the closed string, all negative signs cancel, and we can simply quote the spectrum of the closed string from Ref. 5, Eq. (5.7), by setting $\mu = 0$:

$$(M^{\text{closed}})^2 = 2\pi T_0 (k^2 + l^2) - \frac{2\pi T_0 f}{6} + 4\pi T_0 \sum_{m=1}^{\infty} (\vec{a}_{-m} \cdot \vec{a}_m + \vec{a}'_{-m} \cdot \vec{a}'_m + b_{-m} b_m + b'_{-m} b'_m) , \tag{3.2}$$

where the $\vec{a}_{-m}, \vec{a}'_{-m}$ are transverse coordinate oscillators and b_{-m}, b'_{-m} represent spin excitations with the total spin $S^z = 0$. k and l take the values $0, \pm 1, \pm 2, \ldots$. The total z component of spin for the state is $2k$, and l is a topological quantum number. f is the total number of bosonic degrees of freedom: for four dimensions the two gluon spin

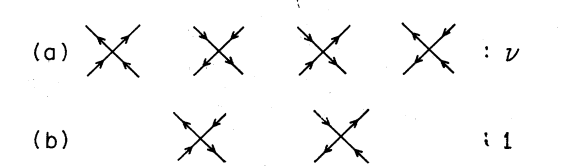

FIG. 5. The vertex weights of the statistical-mechanical F model. The weight ν is an arbitrary parameter.

degrees of freedom are fermionic variables and contribute together only one bosonic degree of freedom. Thus $f = 3$ for four dimensions. The oscillators $\vec{a}_{-m}, \vec{a}'_{-m}$ carry ± 1 units of J_z, the oscillators b_{-m}, b'_m carry none.

The Fock space defined here contains too many states since they are defined with respect to an arbitrary choice for the origin of the σ coordinate of the closed string. The generator for translations in σ is

$$\sum_{n=1}^{\infty} (\vec{a}_{-n} \cdot \vec{a}_n + b_{-n} b_n - \vec{a}'_{-n} \cdot \vec{a}'_n - b'_{-n} b'_n) - kl , \tag{3.3}$$

and only states annihilated by this operator are physical.

Before turning to a detailed analysis of the spectrum of closed strings, we consider the effects of the charge conjugation and parity operations on string states. The states of the field which the fishnet graphs propagate correspond to an oriented sequence of transverse gluons at various points in $\vec{x}_\perp$. The orientation of the sequence may be defined, for example, by following the linking of quark (lower) indices to antiquark (upper) indices of the gluons A_i^j. Under charge conjugation C, each gluon in the state is reproduced with the same spin and $\vec{x}_\perp$ but with phase -1. The orientation of the string is reversed, because quark and antiquark color indices are transposed. Therefore, the topological quantum number l, which was defined in Ref. 2 as a winding number of an effective boson field, is also reversed.

Parity is a little more delicate. This is because the light-cone dynamics do not admit a good parity operator:

$$P(P^{\pm})P^{-1} = P^{\mp} , \tag{3.4}$$

so a "momentum" P^+ is interchanged with the Hamiltonian P^-. However, the intrinsic parity of a state may be determined by its properties under reflection R_0 in the xz plane:

$$R_0 \equiv e^{i\pi J_y} P , \tag{3.5}$$

which leaves P_x, $P^{\pm}$, and $x^{\pm}$ invariant, but reverses the signs of P_y and J_z. A state at rest of spin-parity $|J, m, \pm\rangle$ satisfies

$$R_0 |J, m, \pm\rangle = \pm(-)^{J-m} |J, -m, \pm\rangle . \tag{3.6}$$

Now let us consider the first few states in the closed-string sector. We label the oscillator vacuums by the ket $|k, l\rangle$. The lowest state is for $k = l = 0$, for which $(1/2\pi T_0)M^2 = -f/6$. Since there are an even number of gluons in this state, and no topological quantum number, its charge conjugation is $+1$. Its parity is $+1$, so we have

$$J^{PC} = 0^{++} \quad \text{at} \quad \frac{M^2}{2\pi T_0} = -\frac{f}{6} . \tag{3.7}$$

TABLE I. J^{PC} assignments of the low-lying states of the QCD string.

$\frac{M^2}{2\pi T_0}$	J^{PC}
Closed	
-1	0^{++}
0	$2^{++}, 0^{++}, 0^{+-}$
3	$4^{++}, 3^{--}, 2^{++}, 1^{--}, 0^{++}$
4	$4^{++}, 3^{--}, 2^{++}, 2^{++}, 2^{+-}, 1^{--}, 0^{++}, 0^{-+}$
Open	
$-\frac{1}{4}$	$0^{++}, 0^{-+}, 0^{+-}, 0^{--}$
0	$1^{+-}, 1^{--}$
$\frac{3}{4}$	$2^{++}, 2^{-+}, 2^{+-}, 2^{--}$
1	$2^{++}, 2^{-+}, 0^{++}, 0^{-+}$

The next excited states are $k=\pm1$, $l=0$, and $k=0$, $l=\pm1$. The first states have helicity ±2, even charge conjugation, and even parity. The second have helicity 0, even parity, and opposite charge conjugations. Since there are no helicity ±1 states, Lorentz invariance requires this state to be massless, which would be the case if f were 6 rather than 3.

The higher states (see Table I and Fig. 6) do not seem to have incomplete rotational multiplets even in four dimensions. The connection between the zero-point energy and f is only important when interactions are considered, so for the noninteracting approximation, we may regard the zero-point energy as an adjustable parameter fixed to be 1 by the requirement of Lorentz invariance.

Next we turn to open strings. As we have mentioned, a string may *a priori* terminate on either quarks or gluons. As discussed in Ref. 2, the energy difference between the gluonic open string and the gluonic closed string has a term

$$\frac{1}{a}(\ln N_c g_s^2 - C), \tag{3.8}$$

where C is a pure number. Thus, for $\ln N_c g_s^2 - C > 0$, this energy difference will be infinite as $a \to 0$. Thus, for sufficiently large $N_c g_s^2$, the gluonic open strings will not be in the finite energy spectrum. This is in fact one necessary condition for confinement since the gluonic open strings would have nonet color quantum numbers.

There remains the possibility of terminating the open string on quarks. Since the quark fields are fermionic it is natural to assign quark lines half-integral units of P^+:

$$P^+_{\text{quark}} = (k+\tfrac{1}{2})aT_0, \quad k=0,1,2,\ldots. \tag{3.9}$$

With this choice, the open string diagram in Fig. 7 has the same number of couplings Ng_s^2 per unit time as the closed gluonic string. Thus there will be no $\ln Ng_s^2$ contribution to the open-string–closed-string energy gap. However, a quark bare mass will contribute to the energy gap and can be adjusted so that the $q\bar{q}$ open string has a finite excitation energy above the closed gluonic string. If we assign quark lines integral units of P^+, the gaps will have the $\ln N_c g_s^2$ contribution as well.

The leading quark-gluon coupling is the planar-seagull type coupling shown in Fig. 2. This vertex separately conserves the quark and gluon spin; the

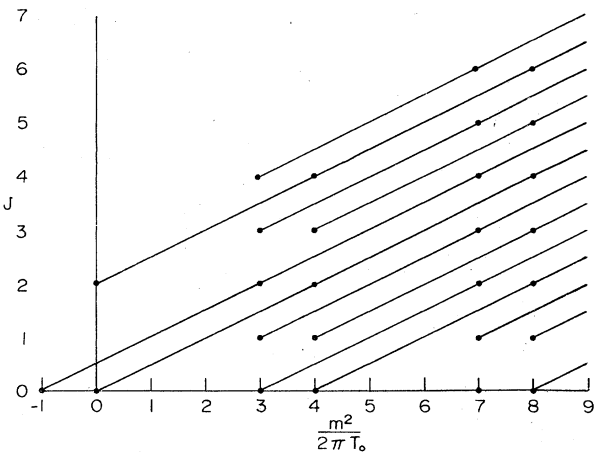

FIG. 6. Closed-string trajectories.

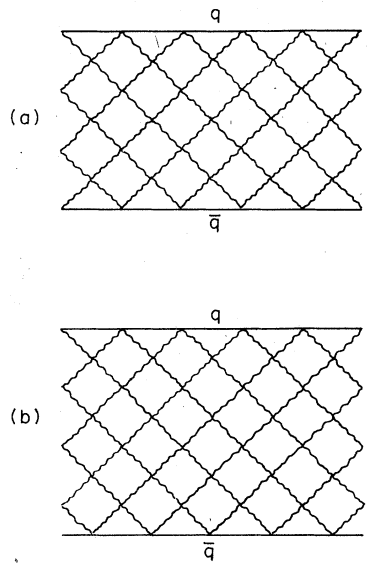

FIG. 7. Open fishnet graphs terminated by $q\bar{q}$ for (a) an even number of gluons and (b) an odd number of gluons.

coupling of a spin-up quark to a spin-up gluon is zero. Thus the boundary condition is that the gluon adjacent to a quark end has its spin antialigned with the quark spin and neither spin flips throughout the diagram.

Just as in Refs. 2 and 5, the simplest way to calulate the open string spectrum is to calculate the partition function and rotate it by 90° so it is a closed-string propagator between definite initial and final states. In the Appendix we use this trick to calculate the open-string spectrum. The resulting spectrum can be summarized by writing

$$(M^{\text{open}})^2 = 2\pi T_0\left(\frac{J^z}{2}\right)^2 - \frac{2\pi T_0 f}{24} + 2\pi T_0 \sum_{m=1}^{\infty} (\vec{a}_{-m}\cdot\vec{a}_m + b_{-m}b_m), \qquad (3.10)$$

where J^z is the total z component of spin including both quarks and gluons:

$$J^z = S^z_{\text{gluon}} + S^z_{q\bar{q}}. \qquad (3.11)$$

According to the arrangement of quark spins, there are four classes of trajectories: ↑↑, ↓↓, ↑↓, ↓↑. Each of these classes contains identical mass spectra and J^z assignments. The parity and charge conjugation assignments will be different, however.

The antiparallel quark spin states occur in an unphysical propagator. The lattice propagator has a factor $(-1)^N$, where N is the number of time steps (see Appendix). In the continuum limit $N\to\infty$, there is a rapid oscillation which may effectively damp out the propagation of these states. We might hope that they will disappear from the finite energy spectrum. However, the correct interpretation of these lattice time oscillations will require a study of the effects of interactions, i.e., a study of $1/N_c$ corrections, which have not yet been pursued. Henceforth we shall restrict our attention to the parallel quark spin states which have good physical propagators.

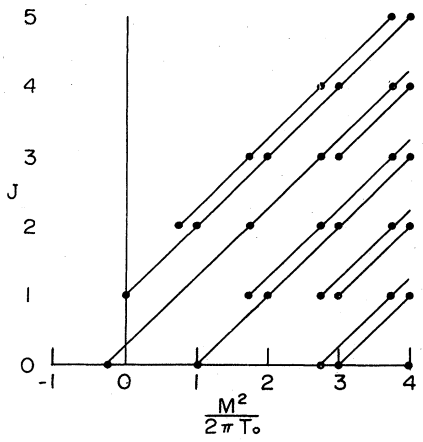

FIG. 8. Open-string trajectories.

There is one more doubling that is a consequence of the structure of the diamond lattice. The fundamental transfer operator spans two time units. As can be seen by inspection of the fishnet graph for an odd number of particles [Fig. 7(b)], any two-step slice is not symmetric under the interchange of roles of the two ends. Since we are interested in the classification of eigenstates of the two-step transfer operator we must distinguish between the $q\bar{q}$ state, where the q is at one end, from the one where it is at the other. Charge conjugation clearly takes the first case into the second. By taking sums and differences of these two states one gets states of opposite charge conjugation. Note that for an even number of particles, the two ends are indistinguishable and this extra doubling does not occur.

The lowest state has $J^z=0$ and no oscillators excited. Since we are considering only $S^z_{q\bar{q}}=\pm1$, we must have $S^z_{\text{gluon}}=\mp1$, and hence an odd number of gluons. Because of the extra doubling for an odd number of particles, the charge conjugates of these states are distinct states. Also the null-plane reflection operator interchanges the two spin configurations. Thus by taking linear combinations, we see that the quantum number assignments of these states is

$$J^{PC}=0^{++},\ 0^{-+},\ 0^{+-},\ 0^{--} \text{ at } \frac{M^2}{2\pi T_0} = -\frac{f}{6}. \qquad (3.12)$$

The first excited states for the open string correspond to $J^z=\pm1$, which can be realized with $S^z_{q\bar{q}}=\pm1$, $S^z_{\text{gluon}}=0$, or $S^z_{q\bar{q}}=\mp1$, $S^z_{\text{gluon}}=\pm2$. Again, Lorentz invariance requires that this state be massless ($f=6$ as in the closed-string case). The charge conjugation of this state is -1 (the gluons are even and the $q\bar{q}$ system odd under C), and it may be easily seen that sums and differences of the two states at fixed J^z have opposite intrinsic parity, thus the assignments

$$J^{PC}=1^{--},\ 1^{+-} \text{ at } \frac{M^2}{2\pi T_0} = 1-\frac{f}{6}=0. \qquad (3.13)$$

We refer the reader to Table I for a listing of quantum number assignments for some of the higher excited states (see also Fig. 8).

We close this section with the observation that these spectrum calculations preserve chiral symmetry. In our approximation, the chiral charge Q_5 is simply proportional to the total quark spin $S^z_{q\bar{q}}$. Thus we can understand the parity doubling as a consequence of chiral symmetry. It is an intriguing possibility that the tachyonic mass of the spin-zero chiral doublet 0^{++}, 0^{-+} may be responsi-

ble for the spontaneous breakdown of this chiral symmetry. If the vacuum is a condensate of the 0^{++} particles, the "pion" 0^{-+} would be a Goldstone boson at zero mass.

IV. CONCLUSION

In this paper we have carried out a calculation of the spectrum of QCD in the dual string approximation following the methods outlined by one of us.[1,2] This approximation is characterized by the limit $N_c \to \infty$ with g_s^2 fixed. The resulting spectrum is that of a heretofore unknown dual string model which we call the QCD dual string. All states lie on linear Regge trajectories. Open strings are terminated by a quark and antiquark, and their Regge trajectories all have the same universal slope $\alpha' = 1/2\pi T_0$. Closed strings have trajectories with slope $\frac{1}{2}\alpha'$. The calculational procedure is not manifestly Lorentz invariant, so it is nontrivial that the spectrum is consistent with Lorentz invariance, even though this consistency demands a massless spin-two particle in the closed-string sector, and massless spin-one states in the open-string sector.

Our limit is also chirally invariant, but this chiral symmetry is realized in a linear way with parity doubling. This linear realization of chirality may be a reflection of an inappropriate bare vacuum, since among the spin-zero tachyons there is a $J^{PC} = (0^{-+}, 0^{++})$ chiral doublet, suggesting that a better vacuum may lead to spontaneous breakdown of chirality.

In addition to the virtues of dual models, our results also share the flaws of previous dual models. We have mentioned tachyons and the graviton-photon problem. Another potential problem is connected with duality. The zero-point energy calculation in the manner of Brink and Nielsen[6,7] is not consistent with Lorentz invariance unless there are three additional sets of boson oscillators over and above the two sets corresponding to transverse coordinate excitations and the one set corresponding to gluon-spin excitations. Thus it is likely that the interactions corresponding to breaking strings will not be consistent with duality unless one increases the number of degrees of freedom, e.g., by increasing the space-time dimension: our $N_c \to \infty$ QCD string does not have a critical dimension of 4.

We, of course, anticipated these dual model problems since our calculational procedure builds in typically "dual model" approximations: most importantly planarity, and the absence of finite momentum constituents—there are only "wee" partons in our limit. Our limit almost certainly enforces the conditions which Mueller has shown lead inevitably to the graviton-photon problem.[15] And then it is hardly surprising that some of the daughter trajectories which have positive intercept have tachyons as their lightest members. Indeed, it is encouraging that the highest trajectories—those of the graviton and photon themselves—do *not* have such tachyons.

Now, having identified in a precise controllable way the "dual limit" of QCD, we may try to identify the features left out of our approximation and to assess whether they have a chance of solving the problems of our limit.

We would like to begin this discussion by returning briefly to the caveat associated with our lattice regularization of the $P^+ = 0$ singularities due to the exchange of longitudinal gluons. As we have mentioned, these singularities are gauge artifacts. When we set up our lattice we simply excluded the troublesome points. We could, for example, have chosen to retain a finite $P^+ = 0$ contribution to the induced four-gluon vertex. Such a choice would not alter Feynman graphs with finite numbers of vertices in the continuum limit, and represents an inherent ambiguity in setting up our lattice version of the field theory. However, such vertices would contribute to the leading fishnet graphs and lead simply to a modification of some of the vertex weights of Fig. 4. The resulting six-vertex model for the spin degrees of freedom has the long-wavelength structure of the anisotropic Heisenberg antiferromagnet, with anisotropy proportional to the strength of the induced vertex. For the closed string, the only place this anisotropy shows up in the spectrum is in the coefficient of the terms k^2 and l^2 [see Eq. (3.2)]:

$$k^2 + l^2 \to (1-\alpha)k^2 + \frac{1}{1-\alpha}\, l^2, \quad |\alpha| < 1 . \tag{4.1}$$

A little experimentation reveals that unless $\alpha = 0$, there are incomplete rotational multiplets at more than one mass value, so one cannot have Lorentz invariance unless $\alpha = 0$. Thus, the $\alpha = 0$ regulation procedure is the only one of this class which gives physically consistent results in the leading-order lattice calculations and is therefore to be preferred. We suspect that the problems of the dual limit are associated with the $N_c \to \infty$ limit itself and not with the regulation procedure we have chosen in order to define this limit.

We turn first to the old "kinematical" problem of the critical dimension. As we have mentioned, duality arguments suggest that we need three more sets of boson oscillators than our limit has allowed to survive. This is certainly an improvement over the 22 extra sets the generalized Veneziano model requires or the nine extra sets the Neveu-Schwarz-Ramond model requires, but it is still not very

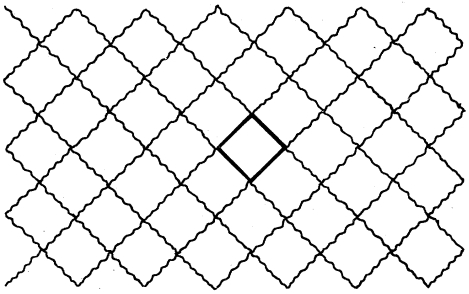

FIG. 9. The insertion of a single quark loop (solid line) in the fishnet.

satisfactory. We suspect the resolution to this problem may be that our limit has frozen out the quark-spin degrees of freedom. The limit $N_c \to \infty$ with N_f/N_c fixed suggested by Veneziano[8] does not have this feature. In this different planar limit, internal fermion loops are included. The oriented color flow orients the quark loops so the only new degree of freedom is the quark helicity. The internal quark loop must close immediately in a single diamond as indicated in Fig. 9. The sum over all flavors enhances the loop by a factor

$$\sum_f e^{-4\pi\alpha' m_f^2} \approx 2.3 \tag{4.2}$$

which is not small compared to 3, the number of colors.

The presence of quark degrees of freedom changes the internal symmetry model from the F model to a more complicated vertex model. There are now four spin states $(\pm 1, \pm \frac{1}{2})$ which couple to each other through the vertices given by the Feynman rules. To our knowledge this model has not yet been solved, but there is a chance that this modified large-N limit will help with the critical dimension problem.

The problems of tachyons, absence of hard-parton structure, and the graviton-photon, may be regarded as dynamical in the sense that we expect their resolution to lie, if at all, in a nonperturbative departure from the dual limit.

It is possible that the tachyons are associated with a bad guess for the bare vacuum. We hope that, starting with a better vacuum, the $1/N_c$ expansion will be well defined, and tachyons will be absent. This resolution has been suggested by Bardakci and Halpern,[16] and is particularly appealing since it could explain the origin of the spontaneous breakdown of chiral symmetry. Since we have at hand the full QCD Hamiltonian, this question may be pursued using variational or other nonperturbative techniques.

On the other hand, the absence of hard-parton structure and the graviton-photon problem, are directly linked to the dual approximation we have made to QCD, and these difficulties will not be resolved without a rather drastic departure from our dual limit. It is helpful in this regard to compare our limit to 't Hooft's $N_c \to \infty$ limit at fixed $N_c g_s^2$ (Ref. 4) (see Fig. 10). Both limits have planar topology and no internal quark loops. In 't Hooft's limit, at least for small $N_c g_s^2$, confinement is lost, but there is a hard-parton description. Our limit is large $N_c g_s^2$ and maintains confinement but loses hard-parton structure. The real hadron structure is undoubtedly determined by intermediate $N_c g_s^2$, which is a very hard region to reach calculationally. Again we may hope that a variational approach guided by both small and large $N_c g_s^2$ results may yield an approximate picture with both confinement and hard partons.[17]

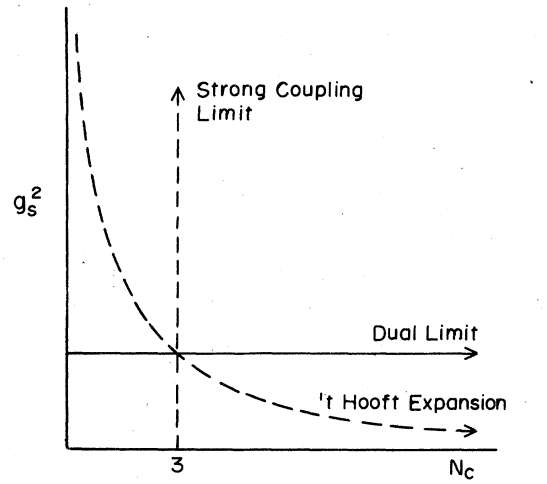

FIG. 10. Three regions of the g_s^2, N_c plane in which the nonperturbative structure of QCD has been studied: the strong-coupling limit (vertical line), the $1/N_c$ expansion of 't Hooft (hyperbola with $g_s^2 N_c = \text{constant}$), and the present dual expansion (horizontal line).

By the same token, one may hope to take nonplanar effects into account. This would give thickness to the string since the gluon quanta can leave the "world sheet" of the planar diagram. We might thereby make contact with bag model phenomenology. The thickness ρ of a long hadron in the bag model[18] is characterized by the bag constant $\rho \sim B^{-1/4}$. In our model the thickness would be characterized by $1/N_c$: $\rho \sim f(1/N_c) T_0^{-1/2}$ with $f(0) = 0$. Thus we expect a relation of the form

$$B = g(N_c)\, T_0^2, \tag{4.3}$$

where $g \to \infty$ as $N_c \to \infty$ and is in principle calculable. We would naturally expect such nonplanar effects to be most important for low-lying states.

It should be mentioned in this context that baryons do not have a simple planar description.

Briefly, the "baryon" state for SU(N_c) must have N_c quarks. Thus, the physically interesting case for baryons is $N_c=3$, for which nonplanar effects presumably cannot be neglected.

ACKNOWLEDGMENTS

We are grateful to L. McLerran for many useful discussions in the early phases of this work and also to M. Peshkin for helpful comments about lattices. We thank J. Shapiro and J. Willemsen for their critical reading of the manuscript. R. C. B. thanks the Center for Theoretical Physics at M.I.T. for their hospitality during the time much of this work was carried out. This work was supported in part by the U. S. Department of Energy under Contract No. EY-76-C-02-3069 and in part by the Alfred P. Sloan Foundation.

APPENDIX: DETAILED CALCULATIONS

A. The spin transfer matrix for the closed string

The propagator for the closed string is represented by the fishnet graph of Fig. 3. Since the four-gluon vertices have no transverse-momentum dependence, the propagator is a product of space-time and color-spin factors. The space-time factor gives the usual transverse excitations of the relativistic string[2]. The color degrees of freedom are frozen out by the $N_c\to\infty$ limit, so that only the spin structure is nontrivial. In this appendix we analyze this spin structure.

We first represent the possible vertices using the S^z basis for the spins of incoming gluons. We use an upward-pointing arrow to indicate spin up, a downward one to indicate spin down. The constraint of spin conservation is just that two arrows enter and two arrows leave each. There are six possible vertices as shown in Fig. 5. The relative weight associated with each vertex is determined from the Feynman rules; those in Fig. 5(a) have weight $v=\frac{1}{2}$, those in Fig. 5(b) have weight -1. The spin factor for the fishnet graph is just equal to the sum over all allowed arrangements of appropriately weighted vertices. This counting problem is identical to the well-known statistical-mechanical F model,[14] which has been studied in this context previously.[5]

This F model may be solved by diagonalizing the corresponding transfer operator. This is the $2^M\times 2^M$ matrix describing the propagation of a row of M spins over a single "time" step and is the lattice analog of the operator $e^{-a\hat{H}}$, where $\hat{H}$ is the Hamiltonian of a one-dimensional quantum-spin system. There are two alternating inequivalent horizontal rows of vertices on the diamond lattice, so we focus on the transfer operator which propagates over two time steps. The amplitude for propagation over N time steps is

$$\langle\psi_f, T=Na \mid \psi_i, T=0\rangle=\langle\psi_f \mid T^{N/2}\mid\psi_i\rangle.$$

During a single time step the gluons interact in independent pairs. The interaction of a pair i, $i+1$ is described by the matrix

$$T_i=\frac{-1+v}{2}+\frac{1+v}{2}+v(\sigma_i^+\sigma_{i+1}^-+\sigma_i^-\sigma_{i+1}^+), \tag{A1}$$

where $\sigma_i^\pm=\frac{1}{2}(\sigma_i^x\pm i\sigma_i^y)$, σ_i^z are Pauli matrices acting on the ith gluon spin. For QCD, $v=\frac{1}{2}$, but we keep the formulas more general. Our vertex weights are not positive definite and do not correspond to physical Boltzmann factors. However, the transfer matrix T_i^0, with weights $+1$, v, is simply related to (A1):

$$T_i=\sigma_i^zT_i^0\sigma_{i+1}^z=\sigma_{i+1}^zT_i^0\sigma_i^z. \tag{A2}$$

The full transfer matrix for two steps is simply a product of factors like (A1). The pairing is always σ_i with σ_{i+1}. In the first step i is odd, in the second i is even:

$$T=\prod_{i\ \text{even}}T_i\prod_{i\ \text{odd}}T_i=\prod_{i\ \text{even}}\sigma_i^zT^0\prod_{i\ \text{even}}\sigma_i^z, \tag{A3}$$

where T_i is the pair transfer matrix involving σ_i and σ_{i+1}, and T^0 has positive-definite weights.

B. Partition functions for open strings in terms of closed-string propagators

By rotating the fishnet for an open-string partition function by 90°, we see that it is identical to a closed-string propagator between definite states. When the open string terminates on quarks, the end gluons are completely polarized and we identify four open strings with end gluon spins ↑↓, ↑↑, ↓↑, ↓↓. The partition functions for the last two are simply related to the first two. One also has different boundary conditions depending on whether the total number of gluons M is even or odd.

Consider first an even number of gluons [Fig. 7(a)]. The partition function $Z_{\text{even}}(\uparrow\downarrow)$ for antiparallel end gluons can be represented, with obvious notation by

$$Z_{\text{even}}(\uparrow\downarrow)=\left\langle\uparrow\downarrow\uparrow\downarrow\cdots\uparrow\downarrow\right|\prod_{i\ \text{odd}}T_i(T)^{M/2-1}\left|\uparrow\downarrow\uparrow\downarrow\cdots\uparrow\downarrow\right\rangle=(-1)^{N/2}\left\langle\uparrow\downarrow\uparrow\downarrow\circ\cdots\uparrow\downarrow\right|\prod_{i\ \text{odd}}T_i^0(T^0)^{M/2-1}\left|\uparrow\downarrow\uparrow\downarrow\cdots\uparrow\downarrow\right\rangle \tag{A4}$$

(where the arrows in the bra and ket vectors denote N spins) whereas the partition function for

parallel end gluons is

$$Z_{\text{even}}(\uparrow\uparrow) = \left\langle \downarrow\uparrow\downarrow\uparrow\cdots\downarrow\uparrow \left| \prod_{i\ \text{odd}} T_i(T)^{M/2-1} \right| \uparrow\downarrow\uparrow\downarrow\cdots\uparrow\downarrow \right\rangle = \left\langle \downarrow\uparrow\downarrow\uparrow\cdots\downarrow\uparrow \left| \prod_{i\ \text{odd}} T_i^0 (T^0)^{M/2-1} \right| \uparrow\downarrow\uparrow\downarrow\cdots\uparrow\downarrow \right\rangle . \tag{A5}$$

The expressions for an odd number of gluons are slightly different:

$$Z_{\text{odd}}(\uparrow\downarrow) = \langle \downarrow\uparrow\downarrow\uparrow\cdots\downarrow\uparrow | T^{(M-1)/2} | \uparrow\downarrow\uparrow\downarrow\cdots\uparrow\downarrow \rangle = (-1)^{N/2} \langle \downarrow\uparrow\downarrow\uparrow\cdots\downarrow\uparrow | (T^0)^{(M-1)/2} | \uparrow\downarrow\uparrow\downarrow\cdots\uparrow\downarrow \rangle , \tag{A6}$$

$$Z_{\text{odd}}(\uparrow\uparrow) = \langle \uparrow\downarrow\uparrow\downarrow\cdots\uparrow\downarrow | T^{(M-1)/2} | \uparrow\downarrow\uparrow\downarrow\cdots\uparrow\downarrow \rangle = \langle \uparrow\downarrow\uparrow\downarrow\cdots\uparrow\downarrow | (T^0)^{(M-1)/2} | \uparrow\downarrow\uparrow\downarrow\cdots\uparrow\downarrow \rangle . \tag{A7}$$

For $M \to \infty$, only the largest eigenvalues of the transfer matrix are important. First imagine diagonalizing the Hermitian operator

$$T_H^0 = \sum_{i\ \text{odd}} (T_i^0)^{1/2} \prod_{i\ \text{even}} T_i^0 \prod_{i\ \text{odd}} (T_i^0)^{1/2}$$

which has the same eigenvalues as T^0:

$$T_H^0 |\lambda\rangle_H = t_\lambda |\lambda\rangle_H$$

and these can be chosen orthonormal. Then the eigenstates of T^0 are

$$|\lambda\rangle = \prod_{i\ \text{odd}} (T_i^0)^{-1/2} |\lambda\rangle_H .$$

The identity may the be resolved:

$$I = \sum_\lambda |\lambda\rangle_{H\,H}\langle\lambda| = \prod_{i\ \text{odd}} (T_i^0)^{1/2} \sum_\lambda |\lambda\rangle\langle\lambda| \prod_{i\ \text{odd}} (T_i^0)^{1/2} . \tag{A8}$$

Using (A8), (A4)–(A7) may be written

$$Z_{\text{even}}(\uparrow\downarrow) = (-1)^{N/2} \sum_\lambda t_\lambda^{M/2-1} \left\langle \uparrow\downarrow\cdots\uparrow\downarrow \left| \prod_{i\ \text{odd}} T_i^0 \right| \lambda \right\rangle \left\langle \lambda \left| \prod_{i\ \text{odd}} T_i^0 \right| \uparrow\downarrow\cdots\uparrow\downarrow \right\rangle , \tag{A4'}$$

$$Z_{\text{even}}(\uparrow\uparrow) = \sum_\lambda t_\lambda^{M/2-1} \left\langle \uparrow\downarrow\cdots\uparrow\downarrow \left| \prod_{i\ \text{odd}} T_i^0 \right| \lambda \right\rangle \left\langle \lambda \left| \prod_{i\ \text{odd}} T_i^0 \right| \uparrow\downarrow\cdots\uparrow\downarrow \right\rangle , \tag{A5'}$$

$$Z_{\text{odd}}(\uparrow\downarrow) = (-1)^{N/2} \sum_\lambda t_\lambda^{(M-1)/2} \left\langle \downarrow\uparrow\downarrow\uparrow\cdots\downarrow\uparrow \middle| \lambda \right\rangle \left\langle \lambda \left| \prod_{i\ \text{odd}} T_i^0 \right| \uparrow\downarrow\cdots\uparrow\downarrow \right\rangle , \tag{A6'}$$

$$Z_{\text{odd}}(\uparrow\uparrow) = \sum_\lambda t_\lambda^{(M-1)/2} \left\langle \uparrow\downarrow\uparrow\downarrow\cdots\uparrow\downarrow \middle| \lambda \right\rangle \left\langle \lambda \left| \prod_{i\ \text{odd}} T_i^0 \right| \uparrow\downarrow\cdots\uparrow\downarrow \right\rangle , \tag{A7'}$$

and we see that only t_λ such that

$$t_\lambda / t_0 = e^{\text{constant}/N}$$

need be considered.

C. The form of Z determined by the Bose-Fermi equivalence

As discussed in Ref. 5, in the continuum limit, $\ln T$ is equivalent to the Hamiltonian for a free boson field defined on a cylinder. Thus one may think of the closed-string propagator as a functional integral:

$$\int D\phi \exp\left[-\frac{T_0}{2} \int_0^T d\tau \int_0^{P^+/T_0} (\dot\phi^2 + \phi'^2) \right] , \tag{A9}$$

where the conditions on ϕ at $\tau = 0$, and $\tau = T$ are appropriate to the initial and final states. In this equivalence, $\dot\phi$ is essentially the spin-wave density. Its integral must assume the quantized values (proportional to the total spin) (with $-\cos\mu = 1 - 1/2v^2$):

$$T_0 \int_0^{P^+/T_0} \dot\phi\, d\sigma = k[2(\pi-\mu)T_0]^{1/2} \quad k = 0, \pm 1, \pm 2, \ldots . \tag{A10}$$

The proportionality factor in (A10) follows from a diagonalization of T^0 using the Bethe ansatz. The quantization (A10) corresponds to a restriction on the admissible wave functionals: they must satisfy

$$\Psi[\phi(\sigma)] = \Psi\left[\phi(\sigma) + \frac{2\pi}{[2(\pi-\mu)T_0]^{1/2}} \right] . \tag{A11}$$

For the closed string, this quantization admits a topological quantum number l, which characterizes the boundary condition at $\sigma = P^+/T_0$:

$$\phi_l(P^+/T_0, \tau) = \phi_l(0,\tau) + \frac{2\pi l}{[2(\pi-\mu)T_0]^{1/2}} \tag{A12}$$

and we must accordingly write (A9) as

$$\sum_l e^{i\theta_l} \int D\phi_l \exp\left[\frac{T_0}{2} \int_0^T d\tau \int_0^{P^+/T_0} d\sigma (\dot\phi_l^{\,2} + \phi_l'^{\,2}) \right] , \tag{A13}$$

where θ_l depends on the initial and final states. Now different l sectors are related by a simple shift of ϕ:

$$\phi_l(\sigma,\tau) = \phi_0(\sigma,\tau) + \frac{2\pi l}{[2(\pi-\mu)T_0]^{1/2}} \frac{\sigma T_0}{P^+} ,$$

and (A13) becomes

$$\sum_l e^{i\theta_l}\exp\left[-\frac{2\pi^2 T_0}{(\pi-\mu)2P^*}\,l^2 T\right]$$

$$\times\int \mathfrak{D}\phi_0 \exp\left[-\frac{T_0}{2}\int_0^T d\tau\int_0^{P^*/T_0} d\sigma(\dot{\phi}_0^{\,2}+\phi_0'^{\,2})\right].$$

(A14)

The Bose-Fermi equivalence does not tell us the phases θ_l, and we must obtain them from the original transfer matrix. All the initial and final states in (A4)–(A7) correspond to locally zero spin-wave density, i.e., they are characterized by $\dot{\phi}_0(\sigma,0)=\dot{\phi}_0(\sigma,T)=0$, and these conditions completely determine the functional integral in (A14). Inspection of (A4′) reveals that each term is positive definite, so for this case, $\theta_l=0$, and the partition function can be immediately written down:

$$Z_{\text{even}}(\uparrow\downarrow)=(-1)^{N/2}x^{-1/24}\sum_{m=-\infty}^{\infty}x^{\pi-\mu/\pi m^2}\prod_{n=1}^{\infty}\frac{1}{(1-x^n)},$$

(A15)

where $x=e^{-\pi N/M}$ and we have dropped bulk and boundary terms. [We remind the reader that in (A15) we have performed the Jacobi-imaginary transformation which effects the rotation back 90°.] To calculate the other partition functions we need to know more about the form of the wave functions.

D. The Bethe ansatz for the diamond lattice

One works within the sector with $m<N/2$ down spins. Denote their locations by x; so a particular state may be represented by

$$|x_1,x_2,\ldots,x_m\rangle.$$

The generalized Bethe ansatz for the eigenfunctions of T is

$$|\lambda\rangle=\sum_P A_P\sum_{x_1<x_2<\cdots<x_m} e^{i(k_{p(1)}x_1+\cdots+k_{p(m)}x_m)}\times\prod_{x_i\,\text{even}}\eta(k_{p(i)})\,|x_1,x_2,\ldots,x_m\rangle,$$

(A16)

where P is a permutation of $1,\ldots,m$. It must be shown that the set of momenta $\{k_j\}$ and the coefficients A_P and phases $\eta(k)$ can be chosen such that $|\lambda\rangle$ is in fact an eigenstate of T. This has been done[14] in the case of a rectangular rather than diamond lattice. The principal new ingredient on the diamond lattices are the phases $\eta(k)$ which reflect the differences in even and odd sites. These phases are determined by the requirement that the transfer operator reproduce the terms in (A16) with down arrows more than three sites apart. The A_P's are determined in such a way that terms with adjacent down arrows are reproduced. The momenta $\{k_j\}$ are constrained by a consistency condition deriving from the overall periodic boundary conditions. The values of η for each set of k's may be obtained by considering an isolated down spin:

$$T^0|x\rangle=\begin{cases}v^{N-2}[|x\rangle+v(|x-1\rangle+|x+1\rangle)+v^2|x+2\rangle], & x\ \text{odd}\\ v^{N-2}[|x\rangle+v(|x-1\rangle+|x+1\rangle)+v^2|x-2\rangle], & x\ \text{even}\end{cases}$$

$$T^0\Big[\sum_{x\,\text{odd}}e^{ikx}|x\rangle+\eta(k)\sum_{x\,\text{even}}e^{ikx}|x\rangle\Big]=v^{N-2}\Big\{(1+v^2e^{-2ik}+2v\eta\cos k)\sum_{x\,\text{odd}}e^{ikx}|x\rangle$$
$$+[2v\cos k+\eta(1+v^2e^{-2ik})]\sum_{x\,\text{even}}e^{ikx}|x\rangle\Big\}+\text{boundary terms}.$$

Thus the interior terms will be reproduced only if

$$\eta^2-2iv\sin k\eta-1=0$$

or

$$\eta=iv\sin k\pm(1-v^2\sin^2 k)^{1/2},$$

with corresponding eigenvalue for T^0:

$$\bar{t}=v^N[\cos k\pm(1/v^2-\sin^2 k)^{1/2}]^2.$$

If we allow k the range $-\pi<k<\pi$, then only one of the solutions for η and $\bar{t}$ need to counted. (They are independent only if $0<k<\pi$.) We pick the + sign:

$$\eta(k)=iv\sin k+(1-v^2\sin^2 k)^{1/2},\qquad\text{(A17)}$$

$$t(k)\equiv[\cos k+(1/v^2-\sin^2 k)^{1/2}]^2.\qquad\text{(A18)}$$

We have divided t by its value on the state with all spins up, namely v^N. That is, t in (A18) is the "excitation" t value for a single spin wave.

For the general case of m down spins the expression (A17) it still true for each k_i, and the "excitation" eigenvalue of the transfer matrix is

$$\prod_{i=1}^{m}[\cos k_i+(1/v^2-\sin^2 k_i)^{1/2}]^2.\qquad\text{(A19)}$$

All the complications are in determining the A_P's and k's in such a way that all boundary effects cancel. In the continuum limit, we do not need to know the solution of this problem in detail because we know so much about the structure of the solution on general grounds. We need only pick out the phases in (A14), and because we know the phases for one case (A15) we only need the relative phases for different choices of boundary conditions.

So let us consider some matrix elements:

$$\left\langle \uparrow\downarrow\uparrow\downarrow\cdots\uparrow\downarrow \middle| \prod_{i\ \text{odd}} T_i^0 \middle| \lambda \right\rangle$$

$$= \langle (\uparrow\downarrow + v\downarrow\uparrow)(\uparrow\downarrow + v\downarrow\uparrow)\cdots(\uparrow\downarrow + v\downarrow\uparrow)\,|\lambda\rangle$$

$$= \prod_i [e^{ik_i}\eta(k_i) + v] f_\lambda(k)\,,$$

$$\left\langle \uparrow\downarrow\cdots\uparrow\downarrow \middle| \prod_{i\ \text{odd}} T_i^0 \middle| \lambda \right\rangle = \prod_i [1 + v\eta(k_i)e^{ik_i}] f_\lambda(k)\,,$$

$$\langle \downarrow\uparrow\downarrow\uparrow\cdots\uparrow\downarrow\,|\lambda\rangle = \prod_i \eta(k_i) e^{ik_i} f_\lambda(k)\,,$$

$$\langle \downarrow\uparrow\downarrow\uparrow\cdots\downarrow\uparrow\,|\lambda\rangle = f_\lambda(k)\,.$$

A little algebra yields

$$e^{ik}\eta(k) + v = e^{ik}[v\cos k + (1 - v^2\sin^2 k)^{1/2}]$$

and

$$1 + v\eta(k)e^{ik} = \eta(k)[v\cos k + (1 - v^2\sin^2 k)^{1/2}].$$

So (A4′)–(A7′) become

$$z_{\text{even}}(\uparrow\downarrow) = (-1)^{N/2}\sum_\lambda t_\lambda^{M/2}\,|f_\lambda|^2\,, \tag{A4″}$$

$$z_{\text{even}}(\uparrow\uparrow) = \sum_\lambda t_\lambda^{M/2}\,|f_\lambda|^2 \prod_i [\eta(k_i)e^{-ik_i}]\,, \tag{A5″}$$

$$z_{\text{odd}}(\uparrow\downarrow) = (-1)^{N/2}\sum_\lambda t_\lambda^{(M-1)/2} \prod_i [v\cos k_i + (1 - v^2\sin^2 k_i)^{1/2}]\,|f_\lambda|^2\,, \tag{A6″}$$

$$z_{\text{odd}}(\uparrow\uparrow) = \sum_\lambda t_\lambda^{(M-1)/2} \prod_i [v\cos k_i + (1 - v^2\sin^2 k_i)^{1/2}]\,|f_\lambda|^2\,. \tag{A7″}$$

The largest eigenvalue t_0 corresponds to the k's distributed between $-(\pi - \mu)$ and $(\pi - \mu)$, for which the factor $[v\cos k + (1 - v^2\sin^2 k)^{1/2}]/v$ is always larger than 1. For low-lying states these factors will always be greater than zero, so we can write unambiguously

$$\prod_i [v\cos k_i + (1 - v^2\sin^2 k_i)^{1/2}] = t_\lambda^{1/2}\,.$$

We finally evaluate the various phases in (A4″)–(A7″). First of all, we recall[5] that

$$\sum_i k_i = l\pi\,,$$

where l is the topological quantum number of (A12). Now

$$\eta(k) = e^{i\sin^{-1}v\sin k}$$

and

$$\prod_i \eta(k_i) = \exp\left(i\sum_i \sin^{-1}v\sin k_i\right).$$

To evaluate this factor we turn to the analysis of Yang and Yang.[19] They use the Bethe ansatz to diagonalize the Hamiltonian for the anisotropic Heisenberg ferromagnet, which has identical eigenstates to the vertex model transfer operator on a rectangular lattice. In the long-wavelength limit, the local structure of this vertex model is isotropic and we therefore expect that in this limit the equations for the k's will be identical to those for the diamond lattice. In their notation, for k's of a low-lying state,

$$\sum_i f(k_i) = \frac{N}{2\pi}\int_{b_1}^{b_2} d\alpha f(k(\alpha))R(\alpha)\,,$$

with b_2 large and b_1 large and negative. $R(\alpha)$ satisfies an equation of the form

$$R(\alpha) = R_0(\alpha) - \left[\int_{b_2}^{\infty} d\beta J_0(\alpha - \beta)R(\beta) + \int_{-\infty}^{b_1} d\beta J_0(\alpha - \beta)R(\beta)\right],$$

where $R_0(\alpha)$ corresponds to the ground state. Then

$$\int_{-\infty}^{\infty} d\alpha f(k(\alpha))R(\alpha) \cong \frac{2\pi}{N}\sum_i f(k_1^0) - \int_{-\infty}^{\infty} d\alpha f(k(\alpha) \times\left[\int_{b_2}^{\infty} d\beta J_0(\alpha - \beta)R(\beta) + \int_{-\infty}^{b_1} d\beta J_0(\alpha - \beta)R(\beta)\right].$$

Now $J_0(x) \sim e^{-c|\alpha|}$ as $\alpha \to \pm\infty$, so we have

$$\int_{-\infty}^{\infty} d\alpha f(k(\alpha))R(\alpha) \cong \frac{2\pi}{N}\sum_i f(k_i^0) - [A_2 f(\pi-\mu) + f(-(\pi-\mu))A_1].$$

So

$$\sum_i [f(k_i) - f(k_i^0)] \cong \frac{N}{2\pi}[f(\pi-\mu)A_2' + f(-(\pi-\mu))A_1'].$$

For our case, $f(k_i) = -f(-k_i)$ and $\sum_i f(k_i^0) = 0 = \sum_i k_i^0$, so we have simply

$$\frac{\sum_i f(k_i)}{\sum_i k_i} \cong \frac{f(\pi-\mu)}{\pi-\mu}$$

or

$$\sum_i f(k_i) \cong f(\pi-\mu) l\pi.$$

Now

$$\sin^{-1} v \sin(\pi-\mu) = \sin^{-1}\left(\frac{1-\cos\mu}{2}\right)^{1/2} = \frac{\mu}{2};$$

hence

$$\prod_i \eta(k_i) \to \exp\left[i\frac{l\pi}{\pi-\mu}\left(\frac{\mu}{2}\right)\right],$$

and so

$$z_{\text{even}}(\uparrow\downarrow) = (-1)^{N/2}\sum_\lambda t_\lambda^{M/2}|f_\lambda|^2,$$

$$z_{\text{even}}(\uparrow\uparrow) = \sum_\lambda t_\lambda^{M/2}|f_\lambda|^2 \exp\left[i\ \frac{l\pi\mu}{2(\pi-\mu)} - l\pi\right],$$

$$z_{\text{odd}}(\uparrow\downarrow) = (-1)^{N/2}\sum_\lambda t_\lambda^{M/2}|f_\lambda|^2 e^{-il\pi},$$

$$z_{\text{odd}}(\uparrow\uparrow) = \sum_\lambda t_\lambda^{M/2}|f_\lambda|^2 \exp\left[+\frac{il\pi\mu}{2(\pi-\mu)}\right].$$

For QCD, $\mu = 0$, and we infer the results quoted in the text.

[1]C. B. Thorn, Phys. Lett. 70B, 85 (1977).
[2]C. B. Thorn, Phys. Rev. D 17, 1073 (1978).
[3]R. Giles and C. B. Thorn, Phys. Rev. D 16, 366 (1977).
[4]G. 't Hooft, Nucl. Phys. B72, 461 (1974).
[5]R. Giles, L. McLerran, and C. B. Thorn, Phys. Rev. D 17, 2058 (1977).
[6]L. Brink and H. B. Nielsen, Phys. Lett. 43B, 319 (1973).
[7]L. Brink and H. B. Nielsen, Nucl. Phys. B89, 18 (1975).
[8]G. Veneziano, Nucl. Phys. B117, 519 (1976).
[9]P. Goddard, J. Goldstone, C. Rebbi, and C. B. Thorn, Nucl. Phys. B56, 104 (1973).
[10]E. Tomboulis, Phys. Rev. D 8, 2736 (1973); A. Casher, Phys. Rev. D 14, 452 (1976).
[11]J. D Bjorken, J. Kogut, and D. E. Soper, Phys. Rev. D 1, 2901 (1970).
[12]R. C. Brower, W. L. Spence, and J. H. Weis, Phys. Rev. Lett. 40, 674 (1978).
[13]It is possible, for example, to introduce a finite $P^+ = 0$ longitudinal exchange on the lattice. This possibility is discussed in Sec. IV.
[14]See, for example, E. H. Lieb and F. Y. Wu, in *Phase Transitions and Critical Phenomena*, edited by C. Domb and M. S. Green (Academic, New York, 1972), p. 331.
[15]A. H. Mueller, Nucl. Phys. B118, 253 (1977).
[16]K. Bardakci, Nucl. Phys. B68, 331 (1974); K. Bardakci and M. B. Halpern, Phys. Rev. D 10, 4730 (1974).
[17]For two-dimensional QCD this blending of soft (Regge) and hard (parton) physics has been studied by R. C. Brower, J. Ellis, M. G. Schmidt, and J. H. Weis, Nucl. Phys. B128, 131 (1977); B128, 175 (1977).
[18]K. Johnson and C. B. Thorn, Phys. Rev. D 13, 1934 (1976).
[19]C. N. Yang and C. P. Yang, Phys. Rev. 150, 321 (1966); 150, 327 (1966).